FLUORESCENCE DYNAMICS OF BODIPY MOLECULES ON ITO THIN FILM

by

Ekrem Yartaşı

B.S., Physics, Anadolu University, 2008

Submitted to the Institute for Graduate Studies in
Science and Engineering in partial fullfilment of
The requirements for the degree of
Master of Science

Graduate Program in Physics

Boğaziçi University

2014

FLUORESCENCE DYNAMICS OF BODIPY MOLECULES ON ITO THIN FILM

APPROVED BY:

Prof. M. Naci İnci (Thesis Supervisor)	. . . . .
Assoc. Prof. M. Burçin Ünlü	. . . . .
Assist. Prof. Heba Yüksel	. . . . .

DATE OF APPROVAL: 17.02.2014

ACKNOWLEDGEMENTS

I would like to express my gratitude to my supervisor Professor M. Naci İnci for his useful comments, remarks, providing the opportunity to work with him and engagement through the learning process of this master thesis.

I would like to thank Miss Gülşen Kösoğlu for her valuable suggestions and my friends Mr Muhammed Hasan Kılınç and Mr Mehmet Yumak for their support during my studies.

I would like to express my gratitudes to Boğaziçi University Research Fund for their support to this research project under the contract number 7384.

Finally, I would like to thank my family, who have supported me throughout the entire process of my education, both by keeping me harmonious and helping me putting pieces together. I will be grateful forever for their love.

ABSTRACT

FLUORESCENCE DYNAMICS OF BODIPY MOLECULES ON ITO THIN FILM

Fluorescence dynamics of bodipy dye molecules deposited on Indium Tin Oxide (ITO) thin films is studied in this thesis. Bodipy molecules deposited on ITO thin films of different thicknesses and resistivities are analyzed by means of lifetimes using time correlated single photon counting technique. Bodipy dyes act as dipoles on the ITO surface. It is envisaged that the electric field of the dipole radiation, which is produced by a bodipy molecule located on a metal planar surface, can be enhanced or inhibited via its image dipole according to the orientation of the prime dipole. The parallel orientation of the bodipy dipole gives rise to enhancement of lifetime since the image dipole's field quenches the field of the prime dipole. This effect results in a considerable enhancement in the dye's lifetime, from 2.57 ns up to 4.76 ns. In addition, it is observed that the resistivity of the films are effective on the emission rates of the bodipy dye molecules rather than the film thickness.

ÖZET

ITO İNCE FİLM ÜZERİNE YERLEŞTİRİLMİŞ BOYA MOLEKÜLLERİNİN IŞIMA DİNAMİĞİ

Bu tezde ITO ince film üzerine yerleştirilmiş boya moleküllerinin ışıma dinamiği incelenmiştir. Boya molekülü dipolünün yaydığı elektrik alan, düz metal yüzey üzerindeki oryantasyonuna göre hayali dipol tarafından yükseltilebilir ya da engellenebilir. ITO ince filmleri üzerine yerleştirilen boya molekülleri zaman korelasyonlu tek foton sayma tekniği kullanılarak elde edilen ışıma ömürleriyle incelendi. Hayali dipol, birincil dipolün alanını engellediği için, boya molekülünün paralel oryantasyonu, ışıma ömründe artışa sebebiyet verdi. Bu etki, 2.57 ns'den 4.76 ns'ye varan bir artışla sonuçlandı. Buna ek olarak, kalınlıktan ziyade, filmin özdirencinin ışıma ömrü üzerinde önemli bir etkiye sahip olduğu gözlemlendi.

TABLE OF CONTENTS

ACKNOWLEDGEMENTS iii
ABSTRACT iv
ÖZET v
LIST OF FIGURES vii
LIST OF TABLES viii
LIST OF SYMBOLS ix
LIST OF ACRONYMS/ABBREVIATIONS x
1. INTRODUCTION 1
2. REVIEW 3
2.1. Fluorescence Process 3
2.1.1. Fluorescence Probes 3
2.1.2. Fluorescence Emission 4
2.2. Fluorescence Lifetime 5
2.2.1. Time-Domain Lifetime Measurement 6
2.2.2. Time Correlated Single Photon Counting (TCSPC) 7
2.3. Quantum Yield 8
2.4. Fluorescence Near Metal Interface 9
2.4.1. Orientation of Dipole 10
2.4.2. Surface Plasmon Polaritons (SPPs) 13
3. EXPERIMENTAL WORKS AND RESULTS 16
3.1. Preparation of ITO thin film + Bodipy 16
3.2. Optical Setup 18
3.2.1. Optical Setup for Fluorescence Spectroscopy 18
3.2.2. Optical setup for fluorescence lifetime measurement 18
3.3. Results 19
3.2.1. Bodipy Spectrum 19
3.2.2. Bodipy Lifetime Measurement 20
4. CONCLUSION 22
REFERENCES 23

LIST OF FIGURES

Figure 2.1. Spontaneous emission. 2

Figure 2.2. Jablonski diagram for photoluminescence [9]. 3

Figure 2.3. Time domain lifetime measurements. 6

Figure 2.4. Illustration of measurement of time difference in TCSPC [10]. 7

Figure 2.5. Principle of TCSPC [8]. 8

Figure 2.6. An arbitrary oriented dipole [9]. 10

Figure 2.7. Parallel and perpendicular dipoles with respect to the surface [14]. 11

Figure 2.8. A spectral overlap. 13

Figure 2.9. (a) Kretschmann and (b) Otto configuration of an Attenuated Total Reflection setup for coupling surface plasmons. 14

Figure 3.1. SEM pictures of the samples. 16

Figure 3.2. Chemical structure of Bodipy. 17

Figure 3.3. Absorption spectrums of the thin ITO films. 17

Figure 3.4. Optical setup of fluorescence spectroscopy. 18

Figure 3.5. Optical setup for fluorescence lifetime measurement. 19

Figure 3.6. Emission spectrum of bodipy. 19

Figure 3.7. Lifetime of free bodipy. 20

Figure 3.8. Lifetime of bodipy deposited on 70nm ITO thin film. 21

LIST OF TABLES

Table 3.1. Resistivity values of all samples. 17

Table 3.2. Lifetimes of all samples. 21

LIST OF SYMBOLS

k_r	Rate constant for radiative deactivation $S_1 \rightarrow S_0$ with emission of fluorescence
k_{nr}	Rate constant for non-radiative deactivation
I	Fluorescence intensity
τ	Lifetime
Φ_F	Quantum yield

LIST OF ACRONYMS/ABBREVIATIONS

MEF	Metal enhanced fluorescence
PMD	Photonic mode density
SERS	Surface enhanced Raman scattering
SPP	Surface plasmon polariton
TCSPC	Time-correlated single photon counting

1. INTRODUCTION

Fluorescence spectroscopy and engineering attempts in altering the decay rate of the fluorescent dye molecules attract the attention of scientists during the recent years for the purpose of a wide range of applications in photonics, material science and biology. Fluorescence spectroscopy and time-resolved fluorescence are considered as research tools for biochemistry and biophysics leading to new methodologies and diverse applications. Such tools are heavily used in biotechnology, flow cytometry, medical diagnostics, DNA sequencing, forensics, and genetic analysis. In addition to these areas, fluorescence imaging for localization and measurement of intracellular molecules by means of fluorescence microscopy [1], sometimes at the level of single-molecule detection [2], can be given as innovative developments. Fluorophores used in the spectroscopy are mostly not hazardous substances on health and have considerably high detectivity. These features bring an alternative to the expense and difficulties of handling radioactive tracers for most biochemical measurements.

A new significant strategy to improve the detection sensitivity and image enhancement is to do it via the amplification of light from fluorophores by coupling them into metal nanostructures. Such a strategy provides the detection of biomarkers, which have low concentrations tagged with fluorescent probes. Another issue is the engineering applications of the metal enhanced fluorescence (MEF). There has been a considerable growth in this area. Surface Enhanced Raman Scattering (SERS), sensors, nanoscopic waveguides for light and nanoscale circuit technology can be counted as innovations, which are brought by MEF [3].

Fluorescence lifetime is an intrinsic property of a chromophore. It means that any change in concentration of the chromophore or its excitation intensity do not alter the lifetime. However, the lifetime change is due to the local environment [4]. The main objective of this thesis is to experimentally show the effect of the parallel orientation of the fluorescent dipole and the resistivity effects on the lifetime of bodipy dye molecules by depositing them on various ITO thin films.

The layout of this thesis is given as follows: fluorescence process and fluorescence lifetime, which include time correlated single photon counting technique used in our experiments for time domain lifetime measurements, is given in Chapter 2. Photon-metal interaction is explained with two subtitles. Beside sample preparation, optical setup for lifetime measurements and fluorescence spectroscopy, emission spectra of bodipy and the lifetime measurement results are presented in Chapter 3. Conclusion and the suggestions for future work is given in Chapter 4.

1. REVIEW

2.1. Fluorescence Process

Photoluminescence consists of two sub-branches which are fluorescence and phosphorescence. It is a photon emission of electronically excited molecule by excitation light, which extends over from ultraviolet to infrared spectra, as turning back to the its ground state. This process is depicted in Figure 2.1.

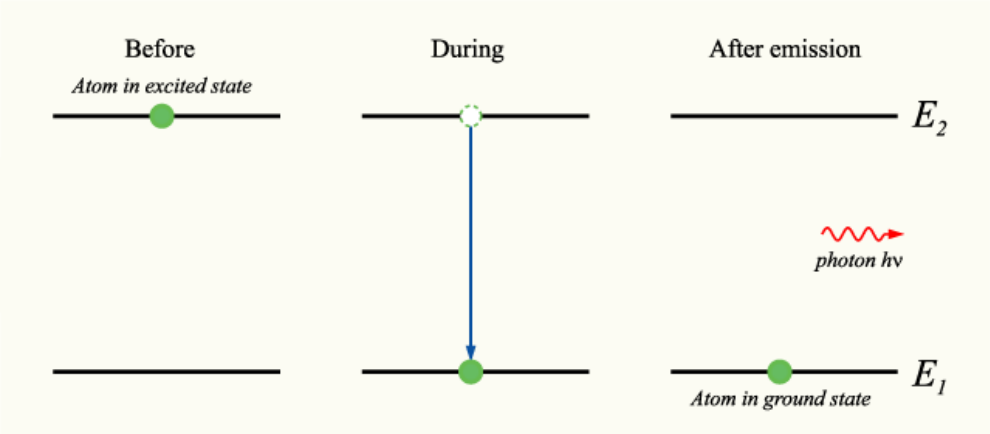

Figure 2.1. Spontaneous emission.

Main difference between fluorescence and phosphorescence (or delayed fluorescence) is that fluorescence is a spontaneous emission whilst phosphorescence is a process in which energy absorbed by a substance is released relatively slowly in the form of light.

Fluorescence process has a vast area of usage especially in biological sciences owing to non-invasive nature. Acquiring the information about labelled macromolecules [5-6], molecular environment and location of molecules in cells [1] can be counted as some of important applications.

These obtained information may be in nanometer or micron scale according to the used setup and technique [7]. Using some environmental parameters such as polarity of the probe, process pressure, temperature, quenchers and ions, fluorescence characteristics of the emitter can be controlled.

2.1.1. Fluorescent Probes

The prominent area of fluorescence spectroscopy is fluorescence probes [8]. Properties of the fluorophore enables to determine the information obtained from the experiments. The wavelength and time resolution which are required for the instruments are also specified by using the spectral properties of the fluorophore. Numerous information in multiple areas such as solid surfaces, living cells, biological membranes, fluoroimmunochemistry, nucleic acids, vesicles, proteins and surfactant solutions can be acquired by the help of the fluorophore.

Fluorescent probes bifurcates into intrinsic and extrinsic fluorescents. Extrinsic fluorophore are added to the sample to provide fluorescence when none exists, or to change the spectral properties of the sample whilst intrinsic ones make emission naturally. Aromatic amino acids, NADH, flavins, derivatives of pyridoxyl, and chlorophyll may be given as several examples to intrinsic fluorophores. Examples for extrinsic ones may be ordered as fluorescein, rhodamine, bodipy and safranin [8].

2.1.2. Fluorescence Emission

The simple and easy way to explain and illustrate photoluminescence phenomena is the Jablonski diagram. In order to analyze the process between the absorption and emission of light singlet ground, first and second electronic states can be defined as S_0, S_1, S_2 respectively.

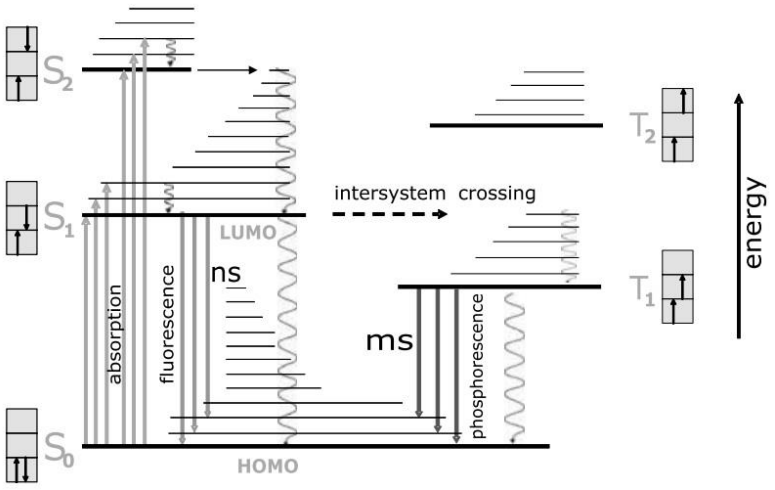

Figure 2.2. Jablonski diagram for photoluminescence [9].

In Figure 2.2, the vertical lines indicate the absorption and emission process among the electronic states. On the other hand, there are many options, which are vibrational states, for the fluorophore to be located at each electronic states. These vibrational states are depicted as the horizontal lines. A fluorophore is excited to higher vibrational level of S_1 or S_2 when it is illuminated with an excitation beam. Then, the molecule turn back to the lowest vibrational level of S_1.

Lifetimes of fluorescence are about $10^{-8}ns$ while this process named as internal inversion takes $10^{-12}ns$ [8]. That is why internal conversion occurs before the fluorescence. Another option to the molecule is spin conversion. Its direction is from S_1 state to the first triplet state T_1 and photon emission from T_1 follows the conversion. The whole process can be named as phosphorescence.

2.2. Fluorescence Lifetime

Fluorescence lifetime or decay time is simply the average time spent by the molecules which are brought to excited state by a pulse of light. These excited molecules can decay to S_0, either radiatively or nonradiatively. Another option for decaying is the intersystem crossing mentioned before.

Intersystem crossing decay route takes remarkably longer time than singlet state decaying, it is about order of millisecond or second. Hence, we shall orientate our attention to singlet state process. Let N be the number of the molecules at the excited state at $t = 0$. The rate of decayed molecules can be written as a differential equation as follows:

$$\frac{dN}{dt} = -(k_r + k_{nr})N \tag{2.1}$$

As shown, this is a basic first order differential equation and its solution has a form of

$$N(t) = N(0)e^{-(k_r+k_{nr})t} \tag{2.2}$$

Where $N(t)$ is the number of molecules in the excited state and $N(0)$ is the number of molecules at $t = 0$. At this stage, the fluorescence lifetime can be defined in terms of the rate constants as follows.

$$\tau = \frac{1}{k_r + k_{nr}} \tag{2.3}$$

So, the solution can be rewritten as in a more common form:

$$N(t) = N_0 e^{-t/\tau} \tag{2.4}$$

On the other hand, in a fluorescence experiment, fluorescence intensity is proportional to the number of molecules still in the excited state at any time t. It is given as follow:

$$I(t) = k_r N_0 e^{-t/\tau} \tag{2.5}$$

$$I_0 = k_r N_0 \tag{2.6}$$

By averaging t over the intensity decay of the molecule, it can be shown that the average time spent between the absorption and emission processes is the lifetime:

$$< t >= \frac{\int_0^\infty tI(t)dt}{\int_0^\infty I(t)dt} = \frac{\int_0^\infty tk_r N_0 e^{-t/\tau}dt}{\int_0^\infty k_r N_0 e^{-t/\tau}dt} \tag{2.7}$$

Results of these integrals are τ and τ^2 in denominator and numerator respectively. As a consequence, the lifetime is the average time of a single exponential decay: $< t >= \tau$.

2.2.1. Time Domain Lifetime Measurement

Time domain fluorescence life time measurement is broadly preferred in fluorescence spectroscopy area such as cellular imaging and studies of biological macromolecules. The other method is frequency domain measurement generally used when luminescent intensity is high. The first one is used in this experiment. In time domain method, the fluorophore molecule is exposed to a short pulse of light and intensity of the emission of the molecule versus time is recorded. Light in the experiment is generally a very short laser beam.

Therefore the lifetime of the molecule whose decay is a single exponential is remarkably longer then the exciting beam. So the lifetime τ of the molecule can directly be

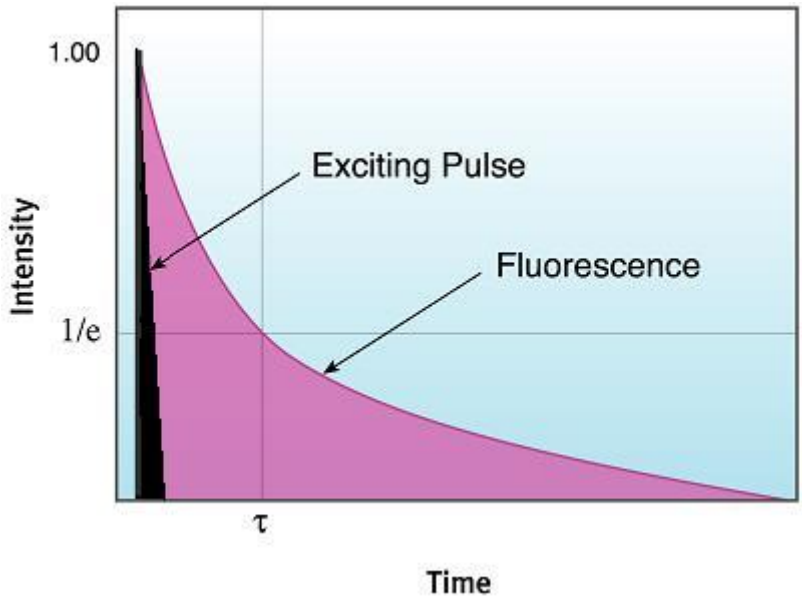

Figure 2.3. Time domain lifetime measurements.

obtained by acquiring slope of the curve of $logI(t)$ versus t [8]. In a real experiment, the observed decay is the convolution integral of the decays from all sharp exciting pulses.

2.2.2. Time Correlated Single Photon Counting (TCSPC)

TCSPC technique is a widely used method in lifetime measurements. Once the fluorophore is excited with a pulse of light, the result is a waveform histogram. TCSPC uses low level high repetition rate signals. Its conditions are adjusted so that the number of photon

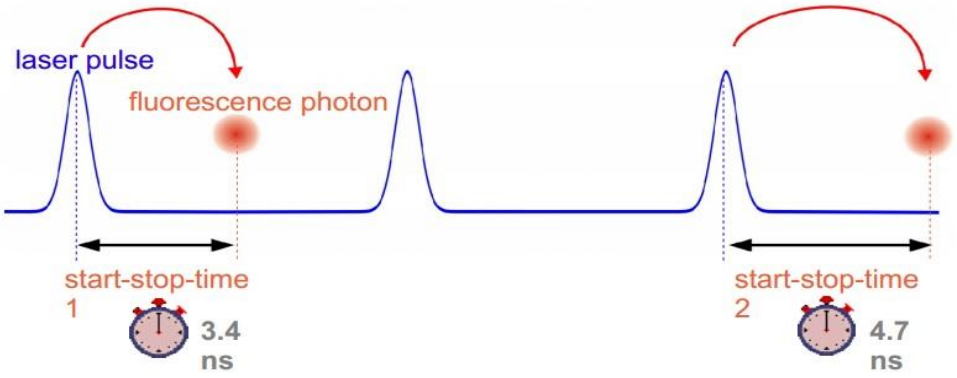

Figure 2.4. Illustration of measurement of time difference in TCSPC [10].

for per light pulse is less than one. In fact, the rate of detection typically 1 photon per 100 pulse of light. Detection times of photons, which are of excitation pulse and observed photons, are stored in a histogram as shown Figure 2.4. TCSPC observes only the first photon. That is why the yielded histogram is waveform of decay [8]. In addition to this, the reason for much less one photon per excitation pulse is that the present electronics is not convenient to measure multiple photon if the lifetime scale is nanosecond.

The basic idea is that once a photon from decay process corresponding to the excitation pulse is detected, the time difference between the excitation pulse and emitted photon is strictly measured via signal. By the way, these signals are obtained with photo multiplier tube (PMT) for emitted photons and with sync circuit for excitation pulse. Then, these time differences are stored in a memory.

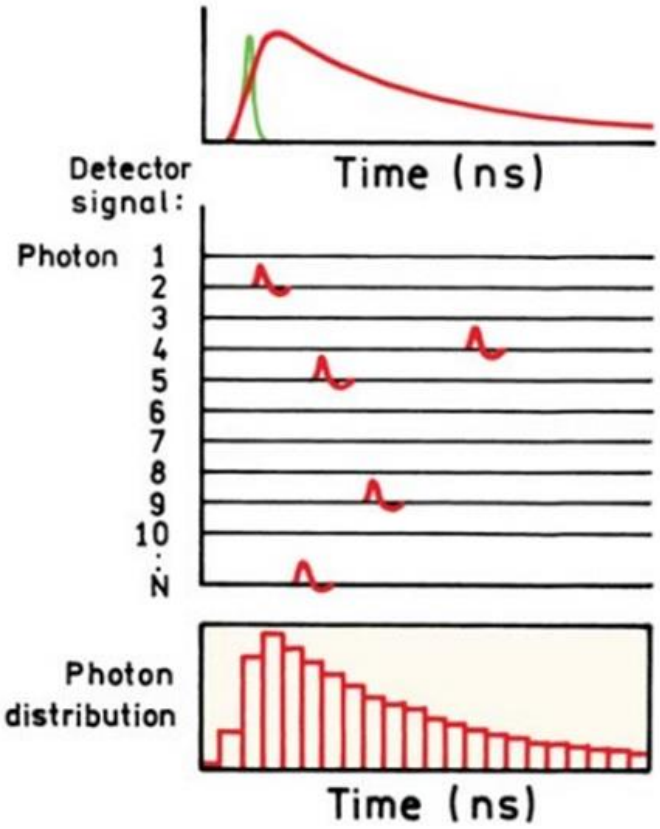

Figure 2.5. Principle of TCSPC [8].

The number of emitted photons (y-axis) versus the time differences (x-axis) is plotted. The yielded histogram is the exponential decay curve. Finally, the curve is fitted to obtain the lifetime [10].

2.3. Quantum Yield

Quantum yield is simply the efficiency of the fluorescence and it can be expressed as ratio of the number of emitted photons to the number of absorbed photons by molecules which are in the ground state:

$$\Phi_F = \frac{number\ of\ photons\ emitted}{number\ of\ photons\ absorbed} \tag{2.8}$$

$$\Phi_F = \frac{k_r}{k_F} = k_r \tau_F \tag{2.9}$$

Maximum and minimum values of the quantum yield are 1 and 0 respectively. It becomes 1 when every molecule in the excited decays and in turn it illuminate, 0 when fluorescence does not exist. As shown in equation, quantum yield is precisely related to k_{nr}, which is nonradiative decay rate constant.

In fact, this constant is an intrinsic property of a particular fluorophore, however, fluorescence lifetime is clearly dependent on k_{nr}. It means that, as mentioned before, the lifetime is sensitive to changes of nonradiative decay rate. Different nonradiative decay routes, which means different k_{nr} values, can be established by altering the surrounding medium of the fluorophore. Any change of it leads to decreasing or increasing of fluorescence lifetime [9].

Quantum yields greater than 1 are possible for photo-induced or radiation-induced chain reactions, in which a single photon may trigger a long chain of transformations. One example is the reaction of hydrogen with chlorine, in which a few hundred molecules of hydrochloric acid are typically formed per quantum of blue light absorbed.

2.4. Fluorescence near Metal Interface

Fluorescence is a typical example of spontaneous emission process. It consists of a process including an emitting atom, which may be molecule or ion, is initially presumed to

be in an excited state. Fluorescence is the result of decaying of the emitter to a lower energy state, which is practically ground state, with a photon. However, it is not necessary that the energy emitted in decaying process is in form of photon, put it another way, it is not need to be a radiation pattern.

There are several nonradiative decay routes which emitting process can follow such as orientation of dipole, surface plasmon polaritons or waveguide modes. According to Fermi's Golden Rule, spontaneous emission rate named Einstein's A_{21} coefficient is given as follow:

$$A_{fi} = \frac{|< f|H|i >|^2 \rho(\upsilon_{fi})}{\hbar^2} \tag{2.10}$$

Here $< f|H|i >$ is the Hamiltonian matrix that connects the excited and lower energy states. $< f|$ and $|i >$ are excited and lower energy states, respectively. $\rho(\upsilon_{fi})$ is the density of photon states at the transition frequency and commonly called Photonic Mode Density (PMD). By modifying the PMD, spontaneous emission process can be manipulated and therefore, fluorescence can be enhanced or inhibited [11-13].

2.4.1. Orientation of Dipole

Consider a fluorophore molecule near a metal surface and let it be illuminated with a pulse of light. Here, arrangement of orientation of dipole molecule can leads an enhancement or inhibition of fluorescence, in other words, the lifetime will be increased or decreased due to alteration of decay rate.

The effect is originating from the image dipole of the fluorophore on metal surface and it appears in small separation regime, i.e., less than 100 nm from a planar metal surface. If the dipole is perpendicular to the metal surface then, field of the image dipole tends to support the strength of the real dipole. When the fluorophore dipole orientation is parallel to the metal surface, this time the image dipole acts as a player cancelling field of the source out, reducing the dipole strength [14].

The cases mentioned above are shown in Figure 2.6. Theoretical explanation of this effect can be built up with standard static image theory. Suppose a primary dipole stands on upper half space of a planar surface with a perpendicular distance z. This is medium 1 and

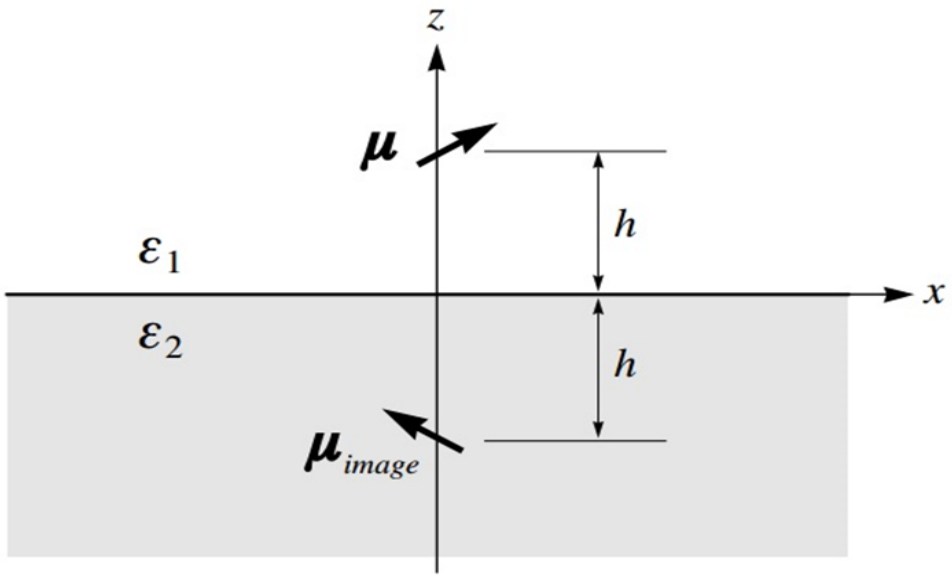

Figure 2.6. An arbitrary oriented dipole [9].

the other is medium 2. The image dipole with the same distance from the surface inner half space has a different electric field magnitude.

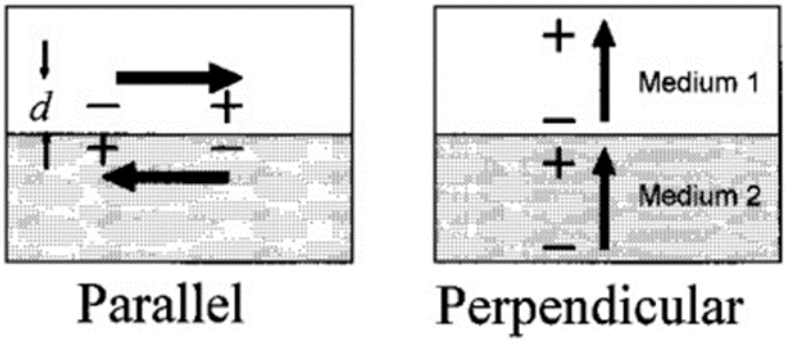

Figure 2.7. Parallel and perpendicular dipoles with respect to the surface [14].

Potential of the real dipole is given as [9]:

$$\boldsymbol{\mu} = \mu_x \boldsymbol{n}_x + \mu_z \boldsymbol{n}_z \tag{2.11}$$

$$\emptyset(\boldsymbol{r}) = \frac{1}{4\pi\varepsilon_0\varepsilon_1}\frac{\boldsymbol{\mu}.\boldsymbol{r}}{r^3} \tag{2.12}$$

Where μ is the dipole moment and for simplicity, it is assumed that this arbitrarily oriented dipole has only vertical and parallel components as shown in Figure 2.6.

For a vertical dipole with $\boldsymbol{\mu} = \mu_z \boldsymbol{n}_z$:

$$\boldsymbol{E}_{prim} = \frac{\mu_z}{4\pi\varepsilon_0\varepsilon_1}\left[\frac{3x(z-h)}{r^5}\boldsymbol{n}_x + \frac{3y(z-h)}{r^5}\boldsymbol{n}_y + \left\{\frac{3(z-h)^2}{r^5} - \frac{1}{r^3}\right\}\boldsymbol{n}_z\right] \tag{2.13}$$

And similar expression for the image dipole:

$$\boldsymbol{E}_{image} = \frac{\mu_z}{4\pi\varepsilon_0\varepsilon_1}\left[\frac{3x(z+h)}{r'^5}\boldsymbol{n}_x + \frac{3y(z+h)}{r'^5}\boldsymbol{n}_y + \left\{\frac{3(z+h)^2}{r'^5} - \frac{1}{r'^3}\right\}\boldsymbol{n}_z\right] \tag{2.14}$$

r' and r are displacement vectors of primary dipole and the image dipole, respectively. Total field of the dipole can be given as:

$$\boldsymbol{E} = \begin{cases} B_v\boldsymbol{E}_{prim}, & z < 0 \\ \boldsymbol{E}_{prim} + A_v\boldsymbol{E}_{image}, & z \geq 0 \end{cases} \tag{2.15}$$

With the boundary conditions at $z = 0$

$$A_v = \frac{\varepsilon_2 - \varepsilon_1}{\varepsilon_2 + \varepsilon_1} \text{ and } B_v = \frac{2\varepsilon_1}{\varepsilon_2 + \varepsilon_1} \tag{2.16}$$

Similar calculations can be done for a horizontal dipole and the results will be:

$$\boldsymbol{E}_{prim} = \frac{\mu_x}{4\pi\varepsilon_0\varepsilon_1}\left[\left\{\frac{3x^2}{r^5} - \frac{1}{r^3}\right\}\boldsymbol{n}_x + \frac{3yx}{r^5}\boldsymbol{n}_y + \frac{3x(z-h)}{r^5}\boldsymbol{n}_z\right] \tag{2.17}$$

$$\boldsymbol{E}_{image} = \frac{\mu_x}{4\pi\varepsilon_0\varepsilon_1}\left[\left\{\frac{3x^2}{r'^5} - \frac{1}{r'^3}\right\}\boldsymbol{n}_x + \frac{3yx}{r'^5}\boldsymbol{n}_y + \frac{3x(z-h)}{r'^5}\boldsymbol{n}_z\right] \tag{2.18}$$

$$\boldsymbol{E} = \begin{cases} B_h\boldsymbol{E}_{prim}, & z < 0 \\ \boldsymbol{E}_{prim} + A_h\boldsymbol{E}_{image}, & z \geq 0 \end{cases} \tag{2.19}$$

$$A_h = -\frac{\varepsilon_2 - \varepsilon_1}{\varepsilon_2 + \varepsilon_1} \text{ and } B_h = \frac{2\varepsilon_1}{\varepsilon_2 + \varepsilon_1} \tag{2.20}$$

As seen in Equation 2.19, total field of any horizontally oriented dipole is quenched due to the fact that $A_v < 0$. Therefore, the primary dipole is driven weakly and this causes decreased fluorescence intensity.

An interesting application of this approximation was performed by Jisha Babu *et al.* [15]. They reported nanoparticle-induced fluorescence lifetime enhancement of a protonated 8-propoxy-quinaldine thiol (PQT) derivative covalently attached to the surface of gold (Au) nanoparticle (AuPQT). They observed a clear enhancement in the lifetime as a result of parallel orientation of the PQT with respect to the Au surface. [15]

Another experiment was performed by Florencio E. Hernandez *et al.* [16]. The chromophore used in the experiment consists of a hybrid system (HS) containing a modified dithiol molecular probe attached to the surface of 5nm average diameter gold nanoshperes (Au-Np).

They took the measurements at room and low temperatures and obtained increased lifetimes by factors of 2 and 3.4 respectively. There was no considerable changing in the fluorescence quantum yield, it means that almost no energy transfer takes place between the molecular probe and the nanoparticle, so it can be concluded that the enhanced lifetimes are only generated by the effect of the parallel orientation.

2.4.2. Surface Plasmon Polaritons

Another issue we can talk about is the Surface Plasmon Polaritons (SPPs) [17]. SPPs are non-radiative modes of the metal-dielectric interfaces and this effect consists of the

coupled oscillation of an electromagnetic field and surface charges at the interface. Because of momentum wave-vector of the mode, which is in the plane of the interface and its field decrease exponentially away from the interface, is always greater than the wave-vector of free photon, it is non-radiative.

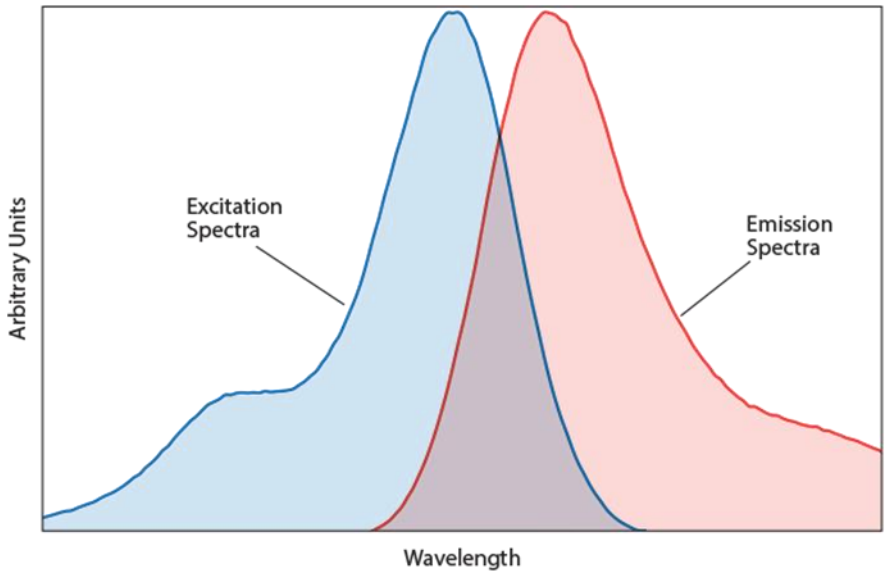

Figure 2.8. A spectral overlap.

SPPs needs an overlap between emission spectrum of the fluorophore and absorption spectrum of the substrate to couple with the emission [18-19]. In addition to this, SPP modes cannot be directly observed, common to all non-radiative decay routes. In order to obtain the coupling, momentum-matching techniques must be used such as prism and grating coupling [4] because of the fact that is needs p-polarized (parallel to the incident plane) waves. SPP coupling gets its maximum, i.e., lifetime quenching, at 20nm separation distance between surface and the fluorophore [20] and coupling of emission field of the fluorophore with evanescent field of SPPs leads to a strongly driven fluorophore [14].

W. L. Barnes *et al.* [21] worked on different structured metal surfaces to manipulate SPP properties of the sample. They show that luminescence emission from a microstructured thin metal film and a planar metal film coated with a microstructured dielectric overlayer is approximately greater than 50 times from a similar planar structure.

R. M. Amos and W. L. Barnes [22] performed an experiment about dependency of spontaneous emission rates of Eu^{+3} to both the distance from, and the thickness of, a silver

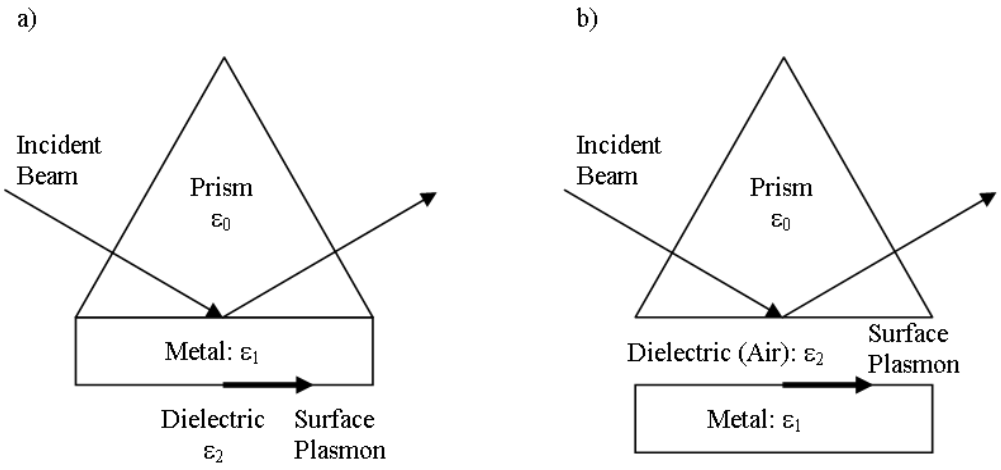

Figure 2.9. (a) Kretschmann and (b) Otto configuration of an Attenuated Total Reflection setup for coupling surface plasmons.

film. The Thickness values which are smaller than 100nm resulted to be obtained additional decay channel which is the SPP on the far side of the metal.

SPP phenomena is seen as next generation of nanoscale circuit technology. Surface plasmon-based circuits, including both SPPs and localized plasmon resonances, have been proposed as a means of overcoming the size limitations of photonic circuits for use in high performance data processing nano devices [23]. The ability to dynamically control the plasmonic properties of materials in these nano-devices is key to their development.

A new approach that uses plasmon-plasmon interactions has been demonstrated recently. Here the bulk plasmon resonance is induced or suppressed to manipulate the propagation of light [24]. This approach has been shown to have a high potential for nanoscale light manipulation and the development of a fully CMOS- compatible electro-optical plasmonic modulator.

2. EXPERIMENTAL

3.1. Preparation of ITO thin film and Bodipy

Indium tin oxide (ITO) is a solid solution of Indium oxide (In_2O_3) and tin oxide (SnO_2), typically, it consists of 90% In_2O_3 and 10% SnO_2 by weight. It has greyish looking in bulk form while it is transparent and colorless when it is coated.

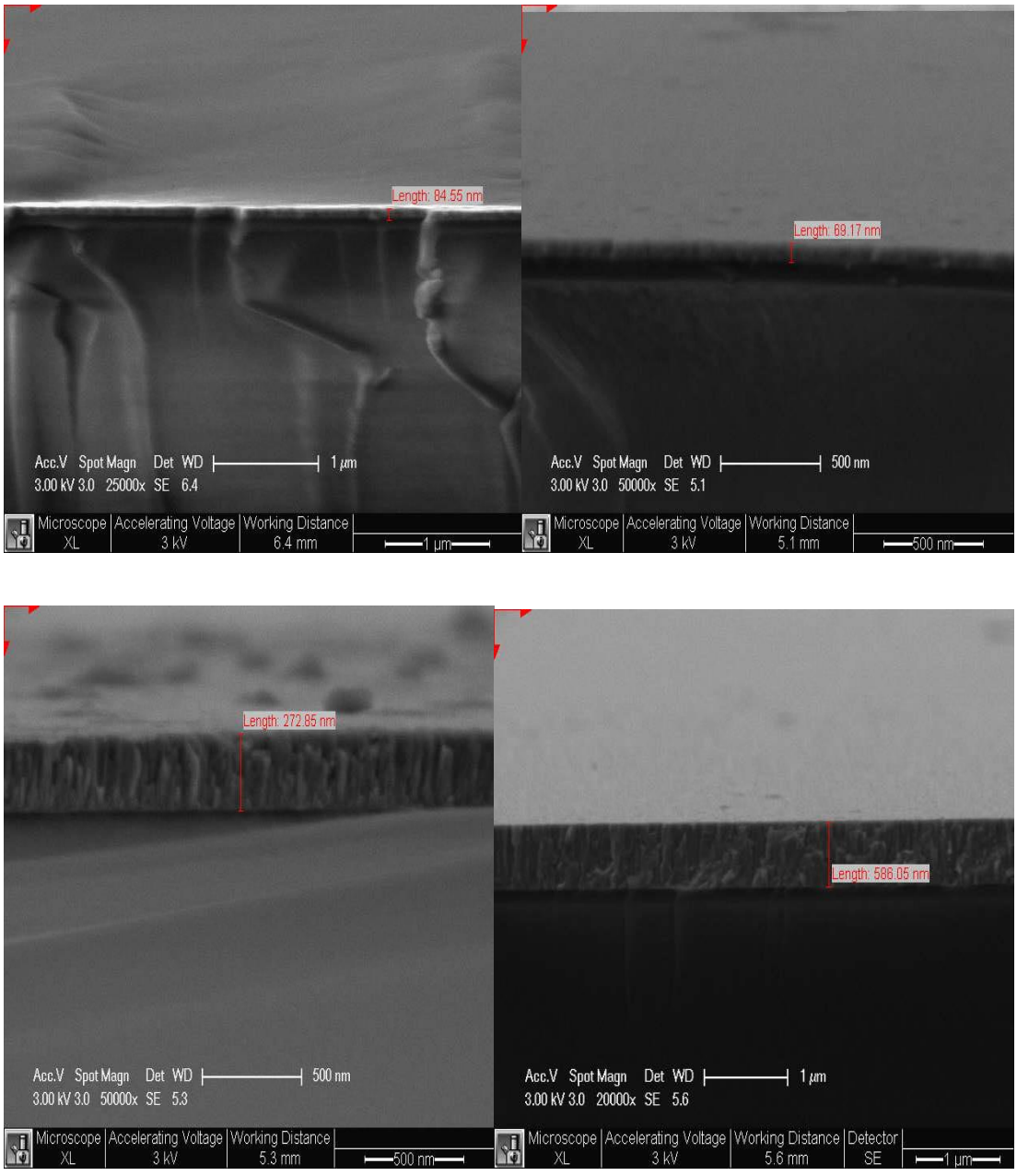

Figure 3.1. SEM pictures of the samples.

These two primary properties of ITO thin film is the top reason for their usage. Four distinct ITO thin films on glass are acquired by sputtering which have 70nm, 80nm, 280nm, and 570nm respectively. SEM pictures of the thin films are shown in Figure 3.1.

A fluorophore having sharp peaks, small Stokes shift [6], high quantum yield is the most desired one in fluorescence experiment by researchers. In this study bodipy (*boron-dipyrromethene*) is used. Bodipy solution of dichloromethane ($30mL/300mL$) is deposed on the surface of the sample by a syringe.

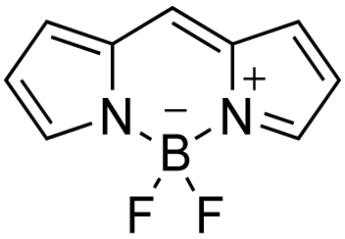

Figure 3.2. Chemical structure of Bodipy.

Spectral behavior of the fluorescent is observed on ITO-glass thin films which have different thickness. Absorption spectra of the ITO thin films are given in Figure 3.3.

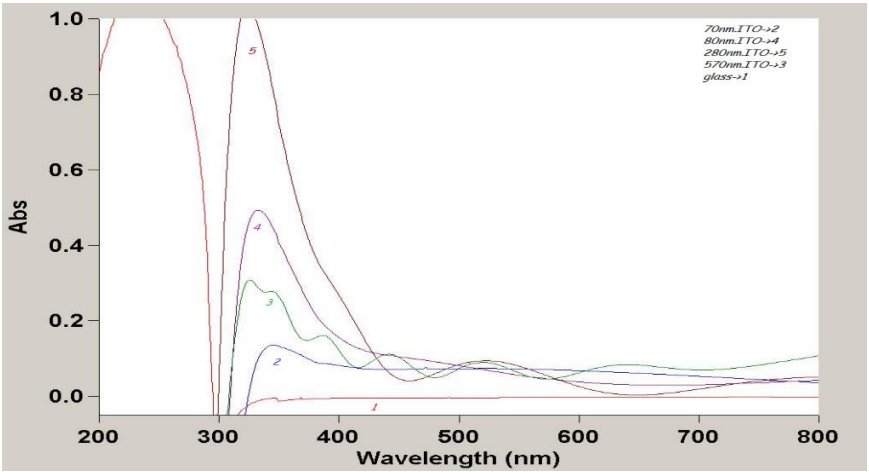

Figure 3.3. Absorption spectrums of the thin ITO films.

Table 3.1. Resistivity values of all samples.

	70nm	80nm	280nm	570nm
Resistivity (ohm.cm)	555×10^{-4}	103×10^{-4}	45×10^{-4}	6×10^{-4}

In addition to the spectrums, Bodipy+ITO thin film structure and resistivity values of thin films are also listed in Figure 3.4. and Table 3.1. respectively.

Figure 3.4. Bodipy+ITO thin film structure.

3.2. Optical Setup

3.2.1. Optical Setup for Fluorescence Spectroscopy

Emission spectrum of bodipy is acquired via the fluorescence spectroscopy setup in which there are the picosecond diode laser (PDL 800-B, PicoQuant), an analyzing computer, a microscope objective (X50 Nikon), a dichroic mirror and the fiber optic spectrometer (Ocean Optics).

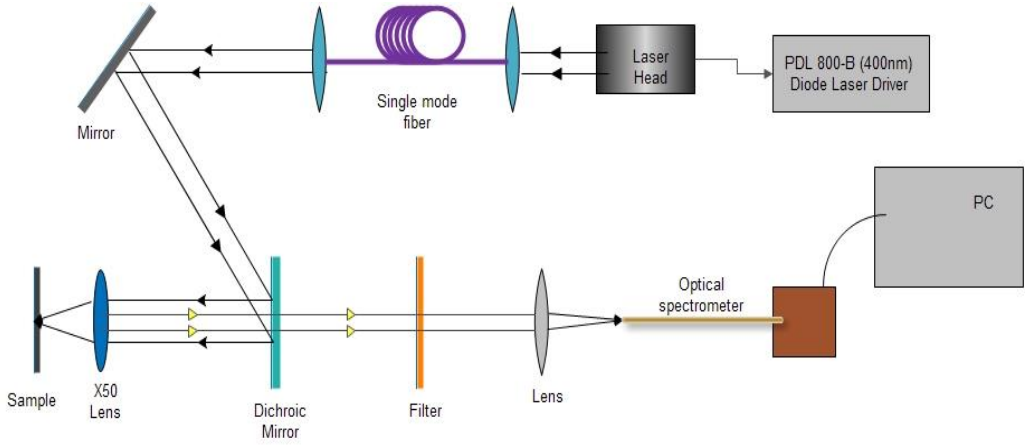

Figure 3.5. Optical setup of fluorescence spectroscopy.

PDL is triggered by an internal oscillator and it is adjustable at 2.5, 5, 10, 20 and 40 MHz Driver unit and head of laser are physically discrete parts and the size of the laser

allows one to place it in any desired location in the setup. Second main instrument is the microscope objective, which is used to focus the excitation laser beam onto the sample. After the excitation of the fluorophore, which emits light at a longer wavelength than that of the excitation light, dichroic mirror and a cutoff filter are used to filter out the fluorescence emission from scattered excitation light. At the end of the path, the fiber optic spectrometer collects the emission photons.

3.2.2. Optical Setup for Fluorescence Lifetime Measurement

Fluorescence lifetime measurement setup is basically the same with the spectroscopy setup except for two differences. The spectrometer altered with photon detector (photomultiplier tube, PMT) and TimeHarp 200 TCSPC, which includes a PCI board and a computer program for monitoring, are added to the setup.

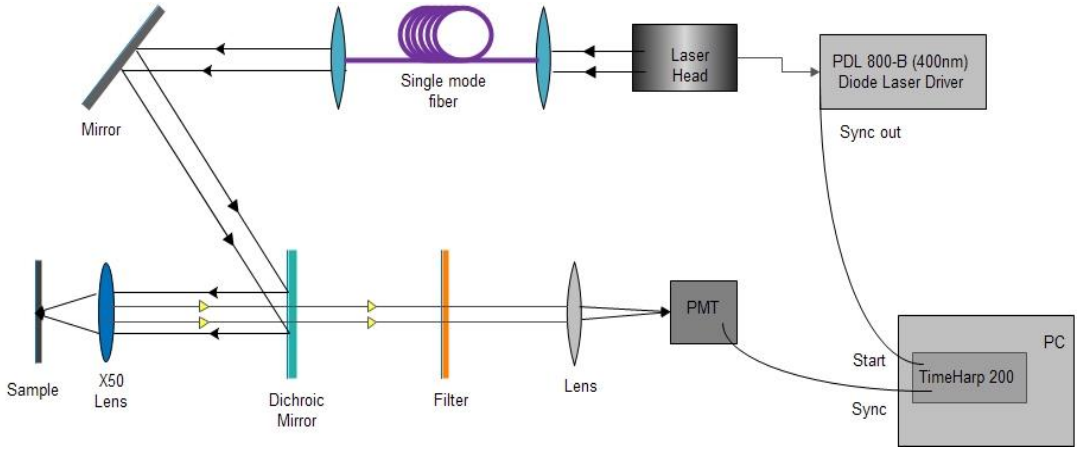

Figure 3.6. Optical setup for fluorescence lifetime measurement

The fluorescence beam following the same route as in the spectroscopy setup arrives the PMT and the data is finally collected and is monitored on TimeHarp 200 pc program.

3.3. Results

3.3.1. Bodipy Spectrum

Fluorescence emission spectra are dependent on both chemical structure of the fluorophore and the solvent in which it is dissolved. In this experiment, dichloromethane is chosen as solvent and the emission spectra is obtained as follows.

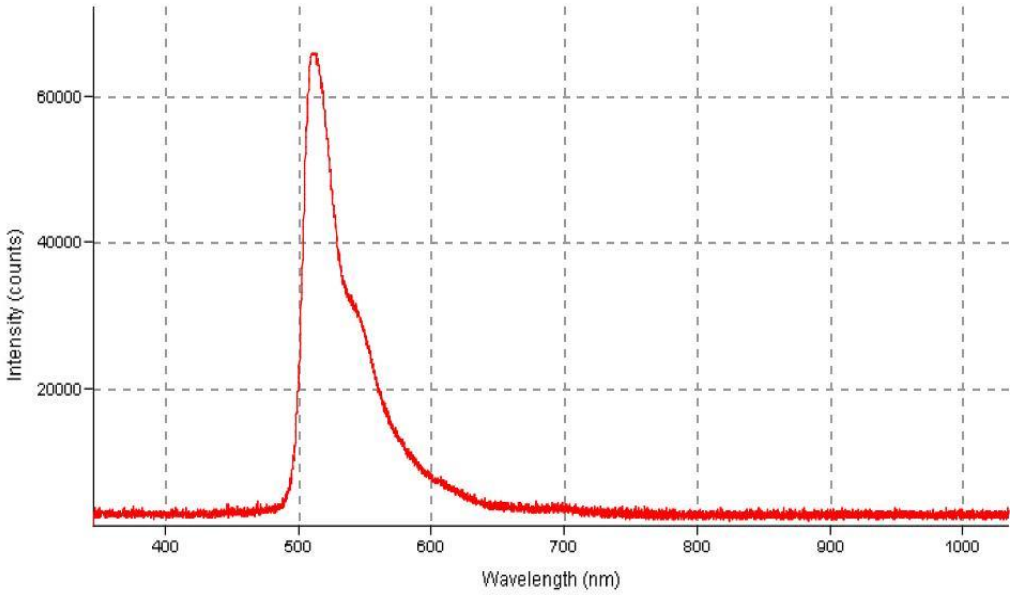

Figure 3.7. Emission spectrum of bodipy dye molecules.

3.3.2. Bodipy Lifetime Measurement

The fluorescence lifetime measurements are performed for each one of the samples, which are free bodipy (on glass) and on different ITO thin films as mentioned before. Acquired data (lifetime histograms) via TimeHarp 200 TCSPC system and its pc program are analyzed in FluoFit decay fitting software package (PicoQuant). The triple exponential fit is preferred to obtain more precise lifetime values. FluoFit software fitted the histograms by using the following formula for different lifetime measurement of bodipy molecules on separate surfaces are performed.

$$I(t) = \sum_{i=1}^{n} A_i e^{-\frac{t}{\tau_i}} \tag{3.1}$$

Free space lifetime of the bodipy molecules is found as $\tau = 2{,}57\ ns$. To observe the effect of the dipole orientation and resistivity, planar metal surfaces with different thickness and resistivity, which are ITO thin films, are used and the lifetimes from the thin film of 70nm and 80nm are measured to be $\tau = 4{,}76\ ns$ and $\tau = 3{,}15\ ns$, respectively. Complete results of the lifetimes for 5 different ITO samples are listed in Table 3.2.

Table 3.2. Lifetimes of all samples.

	Free bodipy	70nm film	80nm film	280nm film	570nm film
Lifetimes (ns)	2.57	4.76	3.15	3.35	2.93

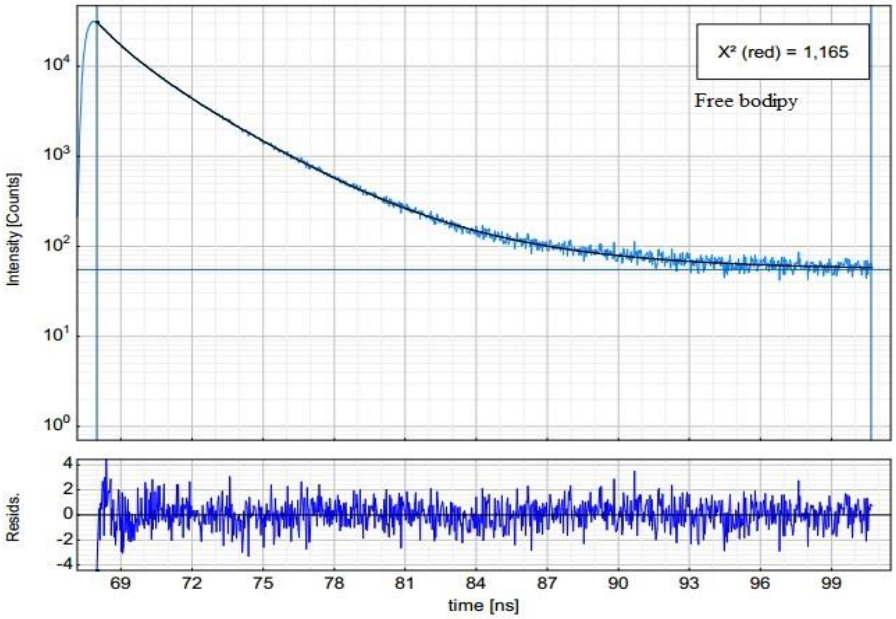

Figure 3.8. Lifetime of free bodipy.

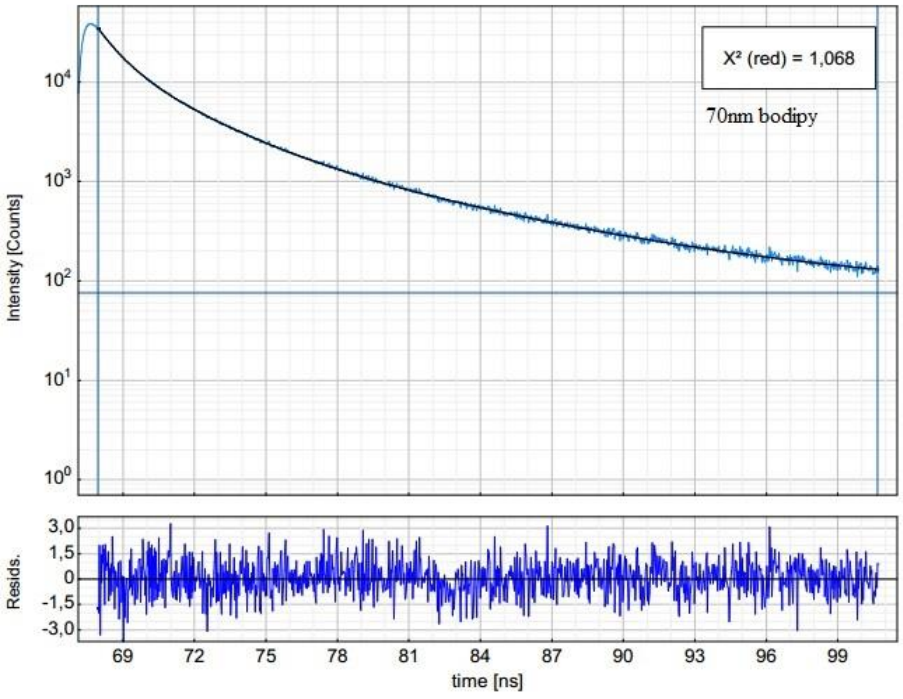

Figure 3.9. Lifetime of bodipy deposited on 70nm ITO thin film.

With these result, effect of the dipole orientation on the decay rate is clearly observed. In this experiment, the lifetime of the bodipy dye molecules, which are deposited onto various ITO thin film, is observed to be enhanced. Thus means that the decay rate is inhibited, owing to parallel dipole orientation of the bodipy molecules with respect to the metal surfaces.

Furthermore, the resistivity of the ITO films seems to be a very important parameter on the decay rate of the dye molecules. For example, the thickness difference between 70 nm and 80 nm samples is only 10 nm. Such a small thickness difference should not be able to cause a significant increase or decrease in the bodipy's spontaneous emission rate. However, our experimental results show that the difference is quite significant, that is, 3.15 ns and 4.76 ns (Table 3.2). We envisage that this difference in the lifetime for 70 ns and 80 ns ITO samples is merely due to the film's resistivity.

3. CONCLUSION

The effect of metal planar surface on fluorescent probe is studied. Spontaneous emission spectra of bodipy dye molecule and absorption spectra for each of four distinct ITO thin films are obtained. Any spectral overlap between the emission and the absorption spectra was not found. This result demonstrates that non-radiative decay rate of the probe does not undergo any modification. Resistivity value of each of the ITO thin film was acquired by means of four point probe. The fluorescent lifetimes are obtained via the time correlated single photon counting technique and the value is acquired as $\tau = 2.57\ ns$.

In order to observe the lifetime change due to orientation of fluorescent bodipy dye molecules, ITO thin films with different thicknesses and resistivities are used. Parallel orientation of the fluorescent dipole resulted in an enhancement in fluorescent lifetime. A modified lifetime up to 4.76 ns is measured for bodipy dye molecules on an ITO planar surface. The significant modification in lifetimes between 70 nm and 80 nm ITO thin films is due to a diverse resistivity between the two samples. This subject shall be studied with many more samples in a future work to resolve the direct effects of the resistivity on the spontaneous emission rate.

REFERENCES

1. Rusanov, A., "Optical Bioimaging and Neuroimaging", *Journal of Biophotonics Special Issue*, Vol. 3, No. 12, pp. 774–783, 2010.

2. Orrit, M., and Bernard, J., "Single Pentacene Molecules Detected by Fluorescence Excitation in a p-terphenyl Crystal", *Physical Review Letters*, Vol. 65, No. 21, pp. 2716–2719, 1990.

3. Darvill, D., Centeno, A., and Xie, F., "Plasmonic fluorescence enhancement by metal nanostructures: shaping the future of bionanotechnology", *Physical Chemistry*, Vol. 15, No. 38, pp. 15709-15726, 2013.

4. Reather, H., *Surface Plasmons*, Springer, Berlin, 1988.

5. Fowler, A.M., Duhamel, J., J. Bahun, G., Adronov, A., Zaragoza-Galán, G., and Rivera, E.. "Studying Pyrene-Labeled Macromolecules with the Model-Free Analysis", *Journal of Physical Chemistry B*, Vol. 116, No. 50, pp. 14689–14699, 2012.

6. Albani, J.R., *Structures and Dynamics of Macromolecules: Absorption and Fluorescence Studies*, Elsevier, 2004.

7. Becker, W., Bergmann, A., *Lifetime Imaging Techniques for Optical Microscopy*, Berlin, Becker & Hickl GmbH, 2003.

8. Lakowicz, J.R., *Principles of Fluorescence Spectroscopy*, Springer, 2006.

9. Novotny, L., Hecht, B., *Principles of Nano-optics*, Cambridge University Press, 2006.

10. Wahl, M., *Time-Correlated Photon Counting Tech Note TCSPC 1.2*, PicoQuant GmbH, 2000.

11. Geddes, C.D., Lakowicz, J.R., "Metal-Enhanced Fluorescence", *Journal of Fluorescence* Vol. 12, No. 2, 2002.

12. Kleppner, D., "Inhibited Spontaneous Emission", *Physical Review Letters*, Vol. 47, No. 4, 1981.

13. Sokolov K., Chumanov G., Cotton T.M., "Enhancement of Molecular Fluorescence near the Surface of Colloidal Metal Films", *Analytical Chemistry* Vol. 70, No. 18, pp. 3898-905, 1998.

14. Barnes, W. L., "Topical Review Fluorescence near Interfaces: the Role of Photonic Mode Density", *Journal of Modern Optics*, Vol. 45, No. 4, 661-669, 1998.

15. Babu, J., George, J. and Varma, R. L., "Metal-induced Fluorescence Lifetime Enhancement of qualdine Chromophore on Gold Nanoparticle Surface", *New Journal Chemistry*, Vol. 37, pp. 2426, 2013.

16. Hernández, F., Yu, S., Garcia, M., "Fluorescence Lifetime Enhancement of Organic Chromophores Attached to Gold Nanoparticles", *Journal of Chemical Physics B*, Vol. 109, No. 19, pp. 9499–9504, 2005.

17. Zhang, J., "Surface plasmon polaritons: physics and applications", *Journal of Physics D: Applied Physics*, Vol. 45, No. 11, pp. 113001, 2012.

18. Chen, Y., Munechika, K., Ginger, D. S., "Dependence of Fluorescence Intensity on the Spectral Overlap between Fluorophores and Plasmon Resonant Single Silver Nanoparticles", *Nano Letters*, Vol. 7, No. 3, pp. 690–696, 2007.

19. P. Haugland, Richard, *Dependence of the Kinetics of Singlet-Singlet Energy Transfer on Spectral Overlap*, Stanford University, 1969.

20. Knobloch, H., Brunner, H., Leitner, A., Aussenegg, F. and Knoll, W., "Probing the Evanescent Field of Propagating Plasmon Surface Polaritons by Fluorescence and Raman Spectroscopies ", *Journal of Chemical Physics* Vol. 98, No. 12, pp. 10093, 1993.

21. Wedge, S. and Barnes, W.L., "Surface Plasmon Polariton Mediated Light Emission through Thin Metal Films", *Optics Express*, Vol. 12, No. 16, pp. 3673-3685, 2004.

22. Amos, R. M. and Barnes, W.L., "Modification of the Spontaneous Emission Rate of Eu^{+3} Ions close to a Thin Metal Mirror ", *Physical Review B*, Vol. 55, No. 11, 1997.

23. Ozbay, E. (2006). "Plasmonics: Merging Photonics and Electronics at Nanoscale Dimensions". *Science*, Vol. 311, No. 5758, pp. 189–193, 2006.

24. Akimov, Yu A; Chu, H S (2012). "Plasmon–plasmon interaction: Controlling Light at Nanoscale". Nanotechnology Vol. 23, No. 44, pp. 444004, 2012.